LBNL-39090
UCM-FT 5/96
July 1996

Higgs physics in the Large N Limit [1]

A. Dobado[2]
Departamento de Física Teórica.
Universidad Complutense de Madrid. 28040 Madrid, Spain

J. Morales
Departamento de Física. Universidad Nacional de Colombia
A.A. 5997 Bogotá, Colombia

J.R. Peláez[3]
Theoretical Physics Group. Lawrence Berkeley Laboratory
University of California. Berkeley, California 94720. USA.

M.T. Urdiales
Departamento de Física Teórica.
Universidad Autónoma de Madrid. 28049 Madrid. Spain

Abstract

In this paper we study the large N limit of the Standard Model Higgs sector with $N\lambda$, Ng^2 and Ng'^2 constant and N being the number of would-be Goldstone bosons. Despite the simplicity of this method at leading order, its results satisfy simultaneously important requirements such as unitarity and the low-energy theorems in contrast with other more conventional approaches. Moreover, it is fully compatible with the Equivalence Theorem and it yields a consistent description of the Higgs boson mass and width. Finally we have also included a phenomenological discussion concerning the applications of this method to the LHC.

PACS: 11.15.Pg, 14.80.Gt

[1]This work was supported by the Director, Office of Energy Research, Office of High Energy and Nuclear Physics, Division of High Energy Physics of the U.S. Department of Energy under Contract DE-AC03-76SF00098.

[2]E-mail:dobado@eucmax.sim.ucm.es

[3] Complutense del Amo fellow. On leave of absence from: Departamento de Física Teórica. Universidad Complutense. 28040 Madrid, Spain. E-mail: pelaez@theor3.lbl.gov, pelaez@vxcern.cern.ch

1 Introduction

As it is well known, the most popular theoretical description of the Symmetry Breaking Sector (SBS) of the Standard Model (SM), is given by the Minimal Standard Model (MSM) which is nothing but an $SU(2)_L \times U(1)_Y$ gauged linear sigma model. Indeed, the hidden sector displays an $SU(2)_L \times SU(2)_R$ *global* symmetry which is spontaneously broken down to $SU(2)_{L+R}$. This mechanism is responsible for the the spontaneous breaking of the *gauge* symmetries of the complete model. In this scheme we have three would-be Goldstone bosons, which will give masses to the W^+, W^- and Z^0 through the Higgs mechanism. They parametrize the space spanned by the three broken generators, i.e. the coset

$$\frac{SU(2)_L \times SU(2)_R}{SU(2)_{L+R}} \simeq \frac{O(4)}{O(3)} \tag{1}$$

There is however a particle which survives the Higgs mechanism, which is known as the Higgs boson. This particle is the only missing piece of the MSM and for this reason it is very important to be able to predict its behaviour in order to confirm or reject the MSM experimentally.

At tree level the dynamics of the Higgs sector is controlled by its self-coupling λ. In fact, its mass is related with this constant by the simple equation $M^2 = 2\lambda v^2$, where $v \simeq 250$ GeV is the vacuum expectation value. Notice that this equation suggests that a heavy Higgs will give rise to a strongly interacting Higgs sector (see [2] for review). However, it should be kept in mind that for large λ the above equation does not hold any more, since perturbation theory is not reliable. As a matter of fact, the tree level amplitudes break unitarity for Higgs masses around 1 TeV [3].

Therefore, it seems clear that a more complex dynamics should emerge for large coupling. At the same time, there are strong hints supporting the triviality of the minimal Higgs sector (see [4] for a review), which means that it should be considered as some kind of effective theory which can be applied only for energies well below some cutoff Λ. In such case, the Higgs mass becomes a decreasing function of this cutoff in such a way that, at some point around 1 TeV, one has $M \simeq \Lambda$. This fact is usually interpreted as an upper bound for the Higgs mass, since it should not be larger than the cutoff Λ of the effective theory.

From the practical point of view the natural place to probe this dynamics is gauge boson scattering. As it is well known, the longitudinal components of the W^+, W^- and Z^0 gauge bosons are related with the three would-be Goldstone bosons. The precise relation is given by the Equivalence Theorem (ET) [5, 3], which states that at high energies the S-matrix elements of longitudinal gauge bosons are the same as those of their corresponding GB. This theorem is very useful since it is far easier to work with the would-be Goldstone bosons than with gauge bosons. The ET has been widely used in many studies concerning the discovery of the Higgs boson at the future Large Hadron Collider (LHC) (see [6] and references therein). With its help and at *lowest order* in the g and g' $SU(2)_L \times U(1)_Y$ gauge couplings, it is possible to reduce the study of longitudinally polarized gauge boson dynamics to the *non-gauged* $O(4)/O(3)$ linear sigma model.

Nevertheless, the tree level, or even the one-loop approximation [7], does not provide a complete description of the expected behaviour of the physical Higgs [8]. This is due to the fact that, in the strong interacting regime, i.e. for large λ, the standard perturbation theory

does not work. In particular it is not able to reproduce properly the position and the width of a heavy Higgs. For this reason some non-perturbative techniques have been studied in the literature like the N/D method (see [3] and [9]) or the Padé approximants [10].

An alternative approach to those listed above is the so called large N limit [11]. The main idea is to extend the $O(4)/O(3)$ symmetry breaking pattern of the linear sigma model to $O(N+1)/O(N)$. Once this is done, the amplitudes are obtained to lowest order in the $1/N$ parameter [12]. The relevant point is that in this simple manner it is possible to study some properties of the Higgs dynamics, which are expected theoretically, but that cannot be reproduced with more conventional techniques. In particular, the would-be Goldstone boson elastic scattering amplitudes are unitary (up to $\mathcal{O}(1/N^2)$ corrections) and satisfy the Weinberg low-energy theorems coming from the $O(N)$ symmetry [13]. Moreover, the Higgs propagator has a pole in the second Riemann sheet that has to be understood as the physical Higgs. The position of this pole is a function of the renormalized Higgs mass M but its real part is never bigger than some value around 1.5 TeV, even in the $M \to \infty$ limit. The fact that there is a saturation value for the Higgs mass is consistent with the assumed triviality of the $O(4)/O(3)$ model and has also been found in other non-perturbative approaches like the above mentioned N/D method or the Padé approximants.

In this work we have applied the large N techniques to an $O(N+1)/O(N)$ linear sigma model which has been gauged with the $SU(2)_L \times U(1)_Y$ symmetry of the SM. The aim of this generalization is twofold. First it will be possible to compute the elastic gauge boson scattering amplitudes *without* using the ET. This is very important since then we can apply our results at low energies too. Nevertheless we show how the ET works remarkably well in the large N approach, which is also a nice check of our computations at high energies. Second, by gauging the linear sigma model, we are able to to include systematically the g and g' corrections keeping at the same time the very good properties of the standard large N limit. We will show that this approach is very easy to implement and for this reason it is appropriate to describe the Higgs phenomenology at the LHC.

The plan of the paper goes as follows. In section two we introduce the $SU(2)_L \times U(1)_Y$ gauged $O(N+1)/O(N)$ linear sigma model. In section three we study the main properties of the physical Higgs boson in this approximation. In the fourth we check our method with the equivalence theorem and how it is satisfied in the large N limit. In the fifth we show our numerical results, which are relevant for the LHC phenomenology. Finally in section six we give the main conclusions of our work.

2 The large N limit of the Higgs sector

We start from the $SU(2)_L \times U(1)_Y$ gauged version of the linear sigma model $SU(2)_L \times SU(2)_R/SU(2)_{L+R} \simeq O(4)/O(3)$ generalized to the coset $O(N+1)/O(N)$. The classical lagrangian is then given by

$$\mathcal{L} = \mathcal{L}_{YM} + \frac{1}{2}(D_\mu \Phi)^T D^\mu \Phi - V(\Phi^2), \tag{2}$$

with $\Phi^T = (\pi^1, \pi^2, ..., \pi^N, \sigma)$ and $\Phi^2 = \Phi^T\Phi$. As usual, $\mathcal{L}_{YM}$ is the standard $SU(2)_L \times U(1)_Y$ Yang-Mills term and the covariant derivatives are defined as

$$D_\mu \Phi = \partial_\mu \Phi - igT_a^L W_\mu^a \Phi + ig' T^Y B_\mu \Phi, \tag{3}$$

where the $SU(2)_L$ and the $U(1)_Y$ generators are $T_a^L = -(i/2)M_a^L$ and $T^Y = -(i/2)M^Y$ with

$$M_1^L = \begin{pmatrix} 0 & 0 & 0 & ... & - \\ 0 & 0 & - & ... & 0 \\ 0 & + & 0 & ... & 0 \\ ... & & & & \\ + & 0 & 0 & ... & 0 \end{pmatrix} \quad , \quad M_2^L = \begin{pmatrix} 0 & 0 & + & ... & 0 \\ 0 & 0 & 0 & ... & - \\ - & 0 & 0 & ... & 0 \\ ... & & & & \\ 0 & + & 0 & ... & 0 \end{pmatrix}$$

$$M_3^L = \begin{pmatrix} 0 & + & 0 & ... & 0 \\ - & 0 & 0 & ... & 0 \\ 0 & 0 & 0 & ... & + \\ ... & & & & \\ 0 & 0 & - & ... & 0 \end{pmatrix} \quad , \quad M^Y = \begin{pmatrix} 0 & + & 0 & ... & 0 \\ - & 0 & 0 & ... & 0 \\ 0 & 0 & 0 & ... & - \\ ... & & & & \\ 0 & 0 & + & ... & 0 \end{pmatrix}.$$

where all the non written entries vanish. The potential is given by

$$V(\Phi^2) = -\mu^2\Phi^2 + \frac{\lambda}{4}(\Phi^2)^2, \tag{4}$$

whose tree level minimum is reached whenever $\Phi^2 = v^2 = NF^2 = 2\mu^2/\lambda$. As a consequence once we choose a vacuum to quantize the theory, the original $O(N+1)$ symmetry will be broken down to $O(N)$. With the standard choice $\Phi_{vac}^T = (0, 0, ..., 0, v)$ and defining the Higgs field as $H = \sigma - v$, we can write

$$V(\pi, H) = -\frac{1}{2}M_H H^2 - \frac{\lambda}{4}(\pi^2 + H^2)^2 - \lambda v H(\pi^2 + H^2), \tag{5}$$

where the tree level Higgs mass is given by $M_H^2 = 2\lambda v^2$.

In order to obtain a well defined perturbation theory, one has to add a gauge fixing and a Faddeev-Popov term to the lagrangian in Eq.2. As far as we are dealing with a gauge theory which is spontaneously broken, it is specially useful to choose an R_ξ gauge, where now π^1, π^2 and π^3 can be directly identified with the would-be Goldstone bosons. With the complete lagrangian at hand it is possible to derive the Feynman rules following the usual procedures. For convenience, we will be working all the time in the Landau gauge, which simplifies the calculations since the ghosts do not couple directly to the π^a fields and their propagator does not have a mass term.

3 The Higgs mass and width

In order to study the main properties of the Higgs resonance in the large N limit of the model defined above, we will start by setting $g = g' = 0$, i.e. we will turn off the gauge interactions. Thus the only fields we have to consider are the N Goldstone bosons π^a and

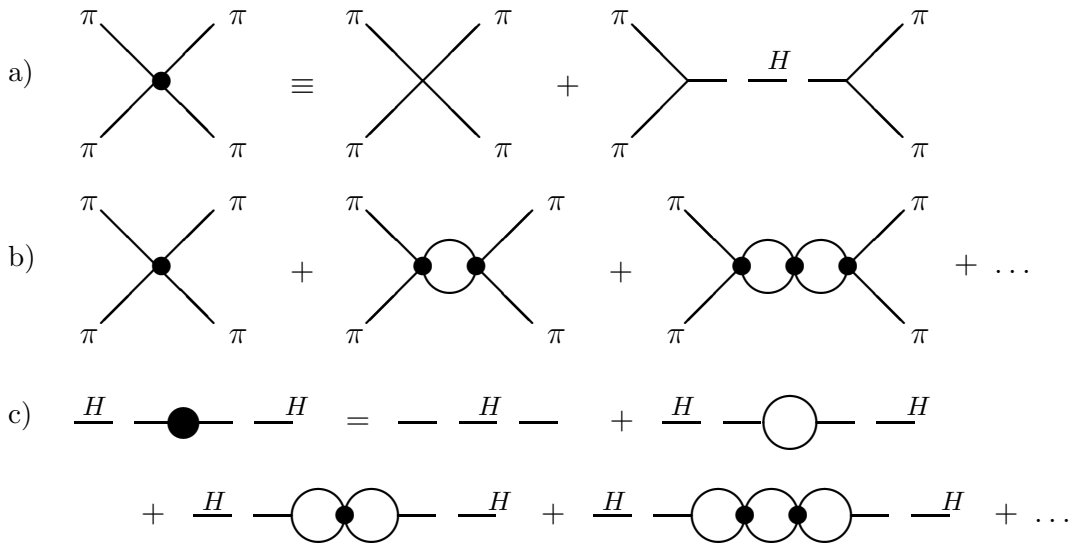

Figure 1: Diagrams contributing to: a) The tree level Goldstone boson scattering amplitude. b) The leading order in the $1/N$ expansion for the same process. c) The Higgs propagator at leading order in the $1/N$ expansion.

the Higgs H. Thanks to the remaining $O(N)$ symmetry as well as to crossing symmetry, the scattering amplitude for the process $\pi^a\pi^b \to \pi^c\pi^d$ can be written as

$$T_{abcd}(s,t,u) = A(s,t,u)\delta_{ab}\delta_{cd} + A(t,s,u)\delta_{ac}\delta_{bd} + A(u,t,s)\delta_{ad}\delta_{bc}. \tag{6}$$

The tree level contributions to the A function (A_0) are obtained from the diagrams in Fig.1.a

$$A_0(s) = -2\lambda\left(1 + \frac{M_H^2}{s - M_H^2}\right) = \frac{s}{NF^2}\frac{1}{1 - s/M_H^2} \tag{7}$$

and therefore they only depend on s. In the large N limit, the relevant diagrams are those shown in Fig.1.b, which are known as bubble diagrams. Each of the loops contributes with the same factor and the sum of all those diagrams can be seen as a geometric series which amounts to

$$A(s) = \frac{s}{NF^2}\frac{1}{1 - s/M_H^2 + sI(s)/2F^2} \tag{8}$$

where the divergent one-loop integral $I(s)$ can be calculated using dimensional regularization. The result is

$$I(s) = \frac{-1}{(4\pi)^2}\left(N_\epsilon + 2 - \log\frac{-s}{\mu}\right), \tag{9}$$

where as usual

$$N_\epsilon = \frac{2}{\epsilon} + \log 4\pi - \gamma_E, \tag{10}$$

and μ is an arbitrary renormalization scale. Thus, in the large N limit the A function only depends on s. The $1/\epsilon$ divergencies appearing in $I(s)$ can be absorbed in the renormalized Higgs mass M_R^2 which can be defined as

$$\frac{1}{M_R^2} \equiv \frac{1}{M_H^2} + \frac{N_\epsilon + 2}{2(4\pi)^2F^2} \tag{11}$$

so that we find

$$A(s) = \frac{s}{NF^2} \frac{1}{1 - \frac{s}{M_R^2} + \frac{s}{2(4\pi)^2 F^2} \log \frac{-s}{\mu^2}} \tag{12}$$

In this approach the Higgs mass is the only parameter that needs renormalization and in particular there is no wave function renormalization. Thus the above amplitude is an observable and μ independent quantity. This fact can be used to find the dependence of the renormalized Higgs mass M_R on the renormalization scale μ which turns out to be

$$M_R^2(\mu) = \frac{M_R^2(\mu_0)}{1 - \frac{M_R^2(\mu_0)}{2(4\pi)^2 F^2} \log \frac{\mu^2}{\mu_0^2}} \tag{13}$$

The renormalized coupling λ_R can be defined in order to keep the tree level relation $M_R^2 = 2\lambda_R N F^2$ and then its running can be easily obtained from the above evolution equation. In practice it is useful to introduce the mass parameter M^2 defined by the equation

$$M^2 = M_R^2(M^2) \tag{14}$$

and then

$$M_R^2(\mu) = \frac{M^2}{1 - \frac{M^2}{2(4\pi)^2 F^2} \log \frac{\mu^2}{M^2}} \tag{15}$$

so that

$$\lambda_R(\mu) = \frac{\lambda(M)}{1 - \frac{N\lambda(M)}{(4\pi)^2} \log \frac{\mu^2}{M^2}} \tag{16}$$

From this formula we can obtain the position Λ of the Landau pole in this approximation which is given by

$$\Lambda^2 = M^2 e^{\frac{(4\pi)^2}{N\lambda(M)}} \tag{17}$$

Therefore, for $g = g' = 0$ the mass parameter is the only free parameter of the model and all the observables can be obtained in terms of it. However, this mass should not be confused with the physical Higgs mass. The physical mass is the mass of the resonance appearing in the scattering channel with the same quantum numbers as the Higgs particle.

In the real world, where $N = 3$, the coset space is $O(4)/O(3) = SU(2)_L \times SU(2)_R / SU(2)_{L+R}$ and thus the interactions are $SU(2)_{L+R}$ symmetric (weak isospin group). Hence there are three Goldstone bosons and the scattering channels can be labelled by the third component of the isospin which can take the values $I = 0, 1, 2$. For an arbitrary N it is still possible to define the appropriate generalization of the above mentioned channels which are then given by [14]

$$\begin{aligned} T_0(s,t,u) &= NA(s,t,u) + A(t,s,u) + A(u,t,s) \\ T_1(s,t,u) &= A(t,s,u) - A(u,t,s) \\ T_2(s,t,u) &= A(t,s,u) + A(u,t,s) \end{aligned} \tag{18}$$

Let us now recall that in Eq.8 we had found that $A(s,t,u) \simeq A(s) \sim \mathcal{O}(1/N)$ and therefore

$$T_0 = NA(s) + \mathcal{O}(1/N) \tag{19}$$

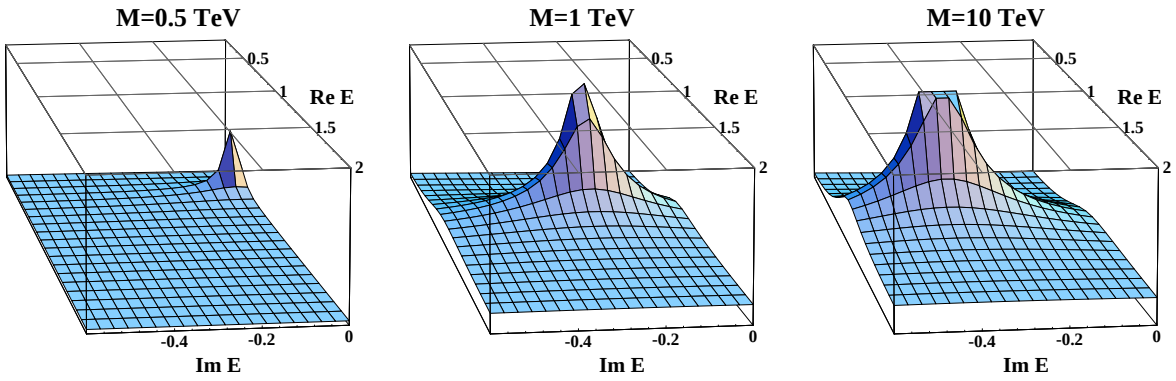

Figure 2: Evolution of the position of the $|t_{00}|$ pole in the $E = \sqrt{s}$ complex plane. We display the lower half of the second Riemann sheet as a function of the M parameter. Notice how the distance to the real axis grows with M, whereas the real part of the position remains bounded. The scale is the same for the three figures.

is the only non zero isospin channel in the large N limit. Fortunately, that is precisely the channel where the Higgs would appear. Customarily the amplitudes are also projected in definite total angular momentum states, leading to partial waves t_{IJ}. It is also obvious that in this case only the t_{00} survives since T_0 only depends on s. Indeed

$$t_{00}(s) = \frac{s}{32\pi F^2}\left(1 - \frac{s}{M^2} + \frac{s}{2(4\pi)^2F^2}\log\frac{-s}{M^2}\right)^{-1} + \mathcal{O}\left(\frac{1}{N}\right) \tag{20}$$

This partial wave has some properties which make the large N limit a sensible approximation to Higgs physics. First, at low energies we find

$$t_{00}(s) \simeq \frac{s}{32\pi F^2} \tag{21}$$

in agreement with the Weinberg low-energy theorems. Second, this partial wave has the correct unitarity cut along the positive real axis of the s variable. Indeed, it can be easily checked that for physical s values, which are located right on the unitary cut where $\log(-s) = \log s - i\pi$, we have

$$\text{Im } t_{00} = \mid t_{00} \mid^2 + \mathcal{O}(1/N) \tag{22}$$

which is the elastic unitarity condition.

Finally, we want to remark that it is possible to find numerically that the partial wave in Eq.20 has a pole in the second Riemann sheet. This pole can be understood as the physical Higgs resonance. In Fig.2 it is shown the position of this pole in the complex plane for different M values.

For low M values the physical Higgs resonance is narrow and the standard Breit-Wigner description of the resonance can be safely applied. Then the physical mass is just given by

M whereas the width is

$$\Gamma = \frac{M^3}{32\pi F^2} \tag{23}$$

which is the tree level result. However, when M increases, the Higgs resonance becomes broader and broader. The pole migrates down in the complex plane and the Breit-Wigner description cannot be used any more. However, the real part of the pole position remains bounded even for very large M as can be seen in Fig.4. This feature is usually called "saturation" and it has also been observed in other non-perturbative approaches to the Higgs dynamics. In particular this behaviour was obtained using the N/D method in [3] and [9], using the Padé approximants in [10] and using the large N limit in [12].

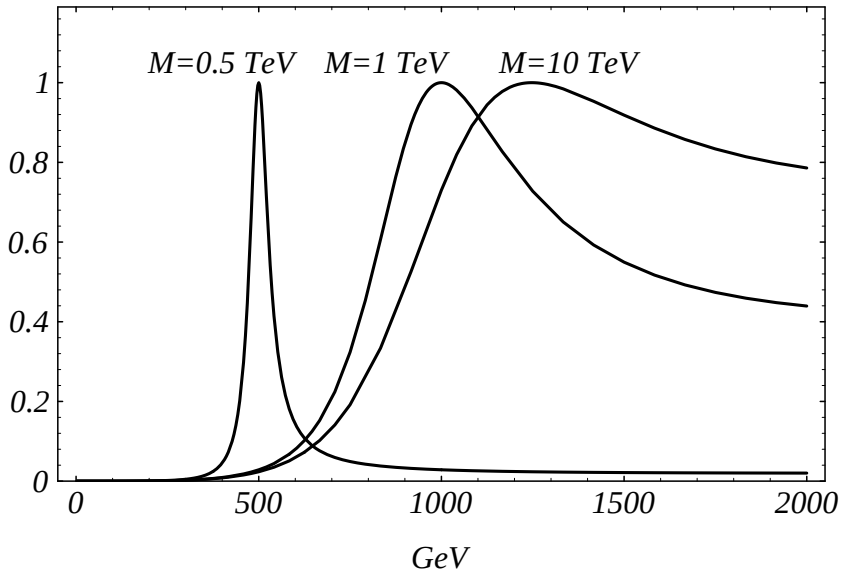

Figure 3: $|t_{00}|^2$ versus $\sqrt{s}$ for different values of the Higgs mass parameter M as defined in Eq.14. Even for values as large as $M = 10$TeV, the position of the resonance is not higher than 1.5TeV.

4 Gauge boson scattering and the Equivalence Theorem

We have already stated that our aim in this work is to study the large N limit of the Higgs sector including the electroweak gauge bosons. More precisely we are considering the $N \to \infty$ limit but keeping Ng^2 and Ng'^2 constant. We will see that such an approach to the gauged Higgs sector turns out to be very useful since it provides a sensible description of gauge boson interactions that still allows easy calculations.

In the following we will concentrate in the elastic scattering process $VV \to VV$ where $V = W^{\pm}, Z^0$. In order to obtain the leading contribution in the approximation defined above, the first observation is that the diagrams at tree level are $\mathcal{O}(g^2)$ (or $\mathcal{O}(g'^2)$). Due to the particular way in which the large N limit has been defined, those graphs are $\mathcal{O}(1/N)$ too. To find the complete set of diagrams contributing to the large N leading order, we have

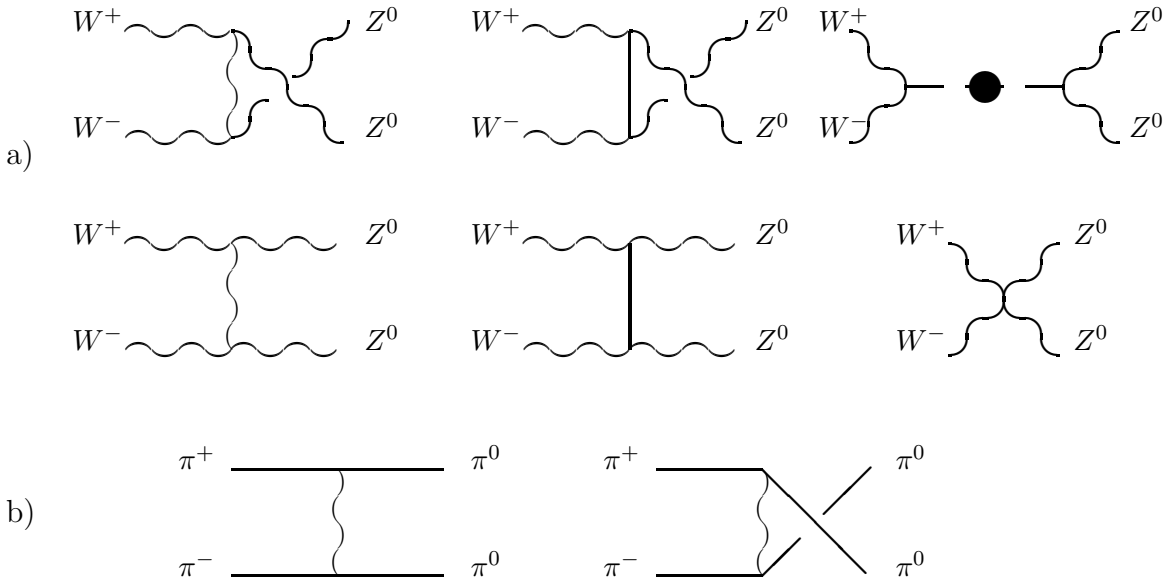

Figure 4: a) Diagrams contributing to the $W^+W^- \to Z^0Z^0$ process at leading order in the $1/N$ expansion. b) Tree level diagrams contributing to the $\pi^+\pi^- \to \pi^0\pi^0$ amplitude containing an internal gauge boson line.

to include into the tree diagrams any possible internal loop without increasing their g^2, g'^2 or $1/N$ power dimensions. It is fairly simple to see that that cannot be accomplished with gauge boson loops. Concerning the scalars, the relevant observation is that gauge bosons are only coupled to the three first π^a, whereas the Higgs interacts with all them. Thus, the only π loops appearing in the large N limit are those coupled to the Higgs field.

The main effect of those π loops is to contribute to the Higgs propagator as it is shown in Fig.1.c. Note that, as far as we are working in the Landau gauge, where all the π fields are massless, many other possible π loop diagrams vanish, since they are proportional to $\int d^{4-\epsilon}q/q^2$ which is zero when using dimensional regularization.

It is not very difficult to calculate the diagrams in Fig.1.c. Using the renormalization prescription of the previous section for the renormalized Higgs mass, we find the Higgs propagator

$$D(q^2) = \frac{1}{q^2 - M_R(-q^2)} + \mathcal{O}\left(\frac{1}{N}\right) \tag{24}$$

where $M_R(-q^2)$ is defined in Eq.15. It is obvious that this $D(q^2)$ has exactly the same pole in the second Riemann sheet than the t_{00} partial wave amplitude in Eq.20, which corresponds to the physical Higgs resonance. At the same time, for small M, we find $M_H(-q^2) \to M$ and thus we recover the standard perturbative (tree level) behavior of the Higgs resonance whose width would then be given by Eq.23. Therefore the above propagator describes properly the Higgs resonances both in the perturbative (light Higgs) and the non-perturbative regime (heavy Higgs).

The most relevant consequence of the previous discussion is that the $VV \to VV$ leading diagrams are just those at tree level, but using the above Higgs propagator instead of that calculated at tree level. For example, the contributions to $W^+W^- \to Z^0Z^0$ can be found in Fig.4.a. Thus in this limit the calculations are not much more difficult than at tree

level. However, the unitarity properties of the large N amplitudes are greatly improved and the Higgs mass and width is properly described in a way which is compatible with other non-perturbative approaches.

An important test for the consistency of the approximation is provided by the Equivalence Theorem (ET). This theorem states that the S-matrix elements of longitudinal electroweak gauge boson are the same as those of their associated would-be Goldstone bosons, up to $\mathcal{O}(m/E)$ corrections, where $m = m_W, m_Z$ and E is the typical C.M. energy of the process. Thus, on the one hand, at high energies the scattering of longitudinal gauge bosons provides information about the Higgs sector of the SM. On the other hand, the ET can be used to calculate the longitudinal gauge boson scattering at high energies in terms of scalars, which are much easier to handle. In fact most of the calculations performed for the LHC until now have used this theorem.

In the approach followed here we are including explicitly the gauge degrees of freedom and therefore we do *not* need to use the ET at all. As a consequence, our approach will be more reliable at lower energies than if we had used the ET, which is neglecting $\mathcal{O}(m/E)$ terms. Nevertheless, the theorem can be useful as a tool to check our results. For example, it relates at high energies the $W^+W^- \to Z^0Z^0$ and the $\pi^+\pi^- \to \pi^0\pi^0$ S-matrix elements. At this moment a few comments are in order. First the S-matrix elements in both sides of the theorem can be expanded in terms of $1/N$ and thus it should apply order by order in $1/N$. In this work we are considering the $N \to \infty$ with λN, $g^2 N$ and $g'^2 N$ constant. In particular that means that for the $\pi^+\pi^- \to \pi^0\pi^0$ process one has to include, at leading order, the diagrams in Fig.4.b in addition to those in Fig.1. This is because in the previous section our model had not been gauged yet, but once it is gauged the new diagrams which are $\mathcal{O}(g^2)$ are also $\mathcal{O}(1/N)$ and they should not be forgotten. these new diagrams are $\mathcal{O}(g^2)$ whereas those considered in the previous sections are simply $\mathcal{O}(1/N)$.

Thus the leading order for this amplitude reads

$$\begin{aligned} T(\pi^+\pi^- \to \pi^0\pi^0) &= \frac{s}{s - M_R^2(-s)} \frac{1}{4(1-x^2) - 4\frac{m_W^2}{E^2} + \frac{m_W^4}{E^4}} \\ &\cdot \left[-4\frac{M_R^2(-s)}{v^2}(1-x^2) + 2g^2(3+x^2) - 2\frac{M_R^2(-s)}{v^2}\frac{m_W^2}{E^2}(5+x^2) \right. \\ &\left. +12\frac{m_W^2}{v^2}\frac{m_W^2}{E^2} - 4\frac{M_R^2(-s)}{v^2}\frac{m_W^4}{E^4} \right] \end{aligned} \tag{25}$$

where $s = 4E^2$, E is the π energy, θ is the scattering angle and $M_R(-s)$ can be obtained from Eq.15. Note that, as far as $-s$ is negative, $M_R(-s)$ produces the imaginary part and the cut for the above amplitude required for unitarity.

After a lengthy but straightforward calculation using the Feynman rules coming from the lagrangian in Eq.2 (plus the standard gauge fixing and Faddeev-Popov terms) and projecting out the longitudinal components, we arrive to the following result for the $W_L^+W_L^- \to Z_LZ_L$ scattering amplitude:

$$T(W_L^+W_L^- \to Z_LZ_L) = \frac{s}{s - M_R^2(-s)} \frac{1}{4(1-x^2) - 4\frac{m_W^2}{E^2}(1-2x^2) + \frac{m_W^4}{E^4}(1-4x^2)}$$

$$\cdot \quad \left[-4\frac{M_R^2(-s)}{v^2}(1-x^2) + 2g^2(3+x^2) + 2\frac{M_R^2(-s)}{v^2}\frac{m_W^2}{E^2}(1-7x^2) \right.$$
$$+4\frac{m_W^2}{v^2}\frac{m_W^2}{E^2}(-14+5x^2) + 8\frac{M_R^2(-s)}{v^2}\frac{m_W^4}{E^4}(1+x^2) + 8\frac{m_W^2}{v^2}\frac{m_W^4}{E^4}(3+x^2)$$
$$\left. -4\frac{M_R^2(-s)}{v^2}\frac{m_W^6}{E^6}(1+2x^2) - \frac{m_W^2}{v^2}\frac{m_W^6}{E^6}(1-4x^2) \right] \qquad (26)$$

As expected, it can be easily checked that these two amplitudes satisfy the ET. One potential problem that could appear when using the ET comes from the different renormalization of the gauge boson and π wave functions [15]. Fortunately, at leading order our $1/N$ expansion does not need wave function renormalization and the ET can be safely applied.

In order to illustrate the above discussion and to check our computational methods we have displayed in Fig.5 the scattering cross section of $W_L^+W_L^- \to Z_L^0Z_L^0$ versus that of $\pi^+\pi^- \to \pi^0\pi^0$. The former is represented by a continuous line whereas the latter has been drawn discontinuously. Notice that to all means and purposes they overlap *at high energies* ($E > 1.2$ TeV).

From Fig.5 we can observe that either with or without the ET, the large N approximation is able to reproduce a well shaped Higgs resonant behaviour and very good high energy properties. The small numerical differences up to almost 1.2 TeV are simply due to the fact that the ET is neglecting the $\mathcal{O}(m/E)$ contributions. Thus we can summarize these two last sections by saying that the large N meets in a very simple way all the known theoretical constraints to the SM Higgs sector, like the low-energy theorems, unitarity, the saturation property and the ET.

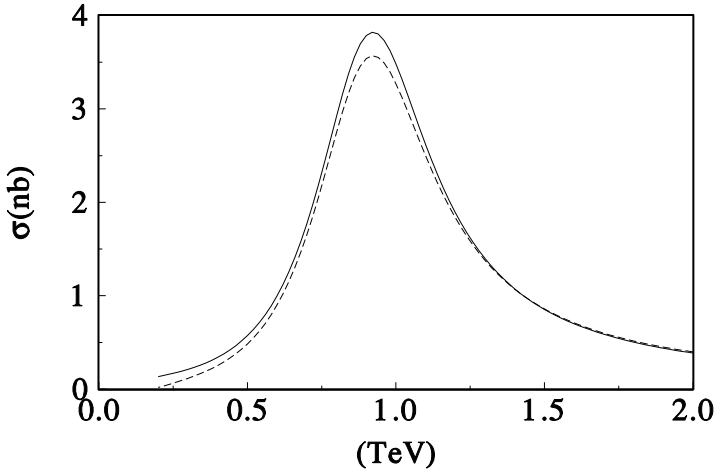

Figure 5: Comparison of the total $W^+W^- \to Z^0Z^0$ cross-section at different $\sqrt{s}$, for $|\cos\theta| < 0.8$, calculated with our large N approach, either with (dashed line) or without the ET (continuous line).

5 Numerical results for the LHC

The main practical application of the approach described above is of course the description of the LHC phenomenology. For this reason it will be used in this section to obtain predictions in terms of the renormalized Higgs mass under the hypothesis that the MSM provides the right model for the electroweak symmetry breaking. In particular we will concentrate on Z^0Z^0 pair production, since this final state is the most sensible to the Higgs resonance properties and at the same time gives rise to a very clear experimental signature.

We consider both final gauge bosons decaying into the cleanest leptonic channels: $Z^0 \to e^+e^-,\ \mu^+\mu^-$. Indeed, we have obtained the number of these events as the total number of Z^0Z^0 pairs times the branching ratio 0.0044. We have computed the total Z^0Z^0 number of events at the LHC with the help of the Monte-Carlo VEGAS code [16]. In order to relate the subprocesses cross sections to the pp initial state, we have used the effective W approximation [17] (which is based on the Weizsaker-Williams approximation [18]) and the MRSD [19] proton structure functions, which are in good agreement with recent experimental results at HERA.

The different subprocesses contributing to Z^0Z^0 production that we have evaluated are

$$\begin{aligned} Z^0Z^0 &\to Z^0Z^0 \\ W^+W^- &\to Z^0Z^0 \\ q\bar{q} &\to Z^0Z^0 \\ gg &\to Z^0Z^0 \end{aligned} \tag{27}$$

All these channels have been calculated using the MSM Feynman rules within the large N limit, which modifies the Higgs boson mass and width according to our previous discussion. Consequently we have used the Higgs propagator given in Eq.24, so that M remains as a free parameter. We have evaluated most of the cross sections shown in Eq.27 at tree level, although gluon-gluon fusion is calculated to one-loop [20], since it occurs via quark loops. As a consequence this cross section is quite sensitive to the top quark mass, that has been set to $m_t = 180$ GeV.

In order to compute the total number of events of the subprocesses in Eq.27 we have set the following expected values for the LHC parameters: the pp center of mass energy, $\sqrt{s} = 14$ TeV and an integrated luminosity $L = 3 \times 10^5 \text{pb}^{-1}$. In addition, we choose the following kinematical cuts on the maximum Z^0Z^0 invariant mass ($\sqrt{\hat{s}}^{\max} = 5$ TeV), the minimum transverse momentum ($p_{tZ}^{\min} = 300$ GeV) and the maximum rapidity $y_Z^{\max} = 2$. Finally, in order to test the dependence on the renormalized mass parameter, we have chosen different input values for M: 100, 500 and 1000 GeV as defined in Eq.14, which cover a wide variety of regimes, from weak to strongly interacting. The results are displayed in Table 1.

6 Conclusions

We have studied the main properties of the Standard Model Higgs sector in the large N limit, i.e. for a large number of would-be Goldstone bosons, including the $SU(2)_L \times U_Y(1)$

	$M = 100$ GeV	$M = 500$ GeV	$M = 1$ TeV
$Z^0Z^0 \to Z^0Z^0$	0.09	2.58	8.95
$W^+W^- \to Z^0Z^0$	21.23	23.39	46.32
$q\bar{q} \to Z^0Z^0$	53.83		
$gg \to Z^0Z^0$	13.42		
$Z^0Z^0 + W^+W^- \to Z^0Z^0$	21.33	25.97	55.27
All$\to Z^0Z^0$	88.57	93.21	122.52

Table 1: Total number of Z^0Z^0 events at LHC decaying to the cleanest leptonic decays (e, μ), in the large N limit of the SM. We have set the following kinematical cuts on the final Z^0 bosons: $\sqrt{\hat{s}}^{\max} = 5$ TeV, $p_{tZ}^{\min} = 300$ GeV, $y_Z^{\max} = 2$. To illustrate the effect of changing the renormalized Higgs mass M in Eq.15, we have chosen three typical values. The contributions from different initial subprocesses are shown explicitly, although those events coming from other gauge boson pairs are listed together. The top quark mass has been fixed to $m_t = 180$ GeV.

interactions, keeping $N\lambda$, Ng^2 and Ng'^2 constant. By using this approximation we have confirmed the expected behaviour from other non-perturbative approaches, both in the weak and the strong interaction regime. In particular the Higgs mass saturation property. In addition we have been able to give a proper description of the Higgs resonance as a pole in the second Riemann sheet of the $I = J = 0$ channel, thus having a well defined width. The corresponding partial wave has very good unitarity properties and it is compatible with the low-energy theorems. Furthermore, the explicit introduction of gauge fields as well as the simplicity to implement this approach allow us, in contrast to most of the previous approaches, to obtain the W^+, W^- and Z scattering amplitudes by means of very simple calculations, even *without* the help of the Equivalence Theorem, which nevertheless has been used to check our results. As an illustration we have applied the large N approximation to estimate the number of Z^0Z^0 events with the cleanest signature at the LHC, including all relevant backgrounds. The results can be found in the table. As it can be seen there, the sensibility of the number of events to the Higgs mass parameter is not very large. However, it could by considerably increased with jet tagging, which could help to separate the more interesting pure fusion events from the background.

We have therefore shown how the large N, despite its simplicity (only the propagator has to be changed), yields a consistent description of the Higgs sector non-perturbative problems, thus improving previous approaches used to obtain predictions for the LHC.

Acknowledgments

This work has been supported in part by the Ministerio de Educación y Ciencia (Spain) (CICYT AEN95-1285-E) and COLCIENCIAS (Colombia). J.R.P would like to thank the Theoretical Group at Berkeley for their kind hospitality, as well as the Jaime del Amo Foun-

dation for a fellowship. Partial support by US DOE under contract DE-AC03-76SF00098 is gratefully acknowledged.

References

[1] S. L. Glashow, *Nucl. Phys.* **22** (1961) 579
S. Weinberg, *Phys. Rev. Lett.* **19** (1967) 1264
A. Salam, *Proc. 8th Nobel Symp.,* ed. N. Svartholm, p. 367, Stockholm, Almqvist and Wiksells (1968)

[2] M.S. Chanowitz, *Ann. Rev. Nucl. Part. Sci.* **38** (1988) 323

[3] B.W. Lee, C. Quigg and H. Thacker, *Phys. Rev.* **D16** (1977)

[4] D.J.E. Callaway, *Phys. Rep.* **167** (1988) 241

[5] J.M. Cornwall, D.N. Levin and G. Tiktopoulos, *Phys. Rev.* **D10** (1974) 1145
C.E. Vayonakis, *Lett. Nuovo Cim.* **17** (1976) 383
M.S. Chanowitz and M.K. Gaillard, *Nucl. Phys.* **B261** (1985) 379
G.K. Gounaris, R. Kogerler and H. Neufeld, *Phys. Rev.* **D34** (1986) 3257

[6] J. Bagger et al., *Phys. Rev.* **D52** (1995) 3878

[7] S. Dawson and S. Willenbrok, *Phys. Rev. Lett.* **62** (1989) 1232
M.J.G. Veltman and F.J. Yndurain, *Nucl. Phys.* **B325** (1989) 1

[8] G. Valencia and S. Willenbrock, *Phys. Rev.* **D46** (1992) 2247

[9] K. Hikasa and K. Igi, *Phys. Rev.* **D48** (1993) 3055

[10] A. Dobado, M.J. Herrero and T.N. Truong, *Phys. Lett.* **B235** (1990) 134
A. Dobado *Phys. Lett.* **B237** (1990) 457
S. Willenbrock, *Phys. Rev.* **D43** (1991) 1710
D.A. Dicus and W.W. Repko, *Phys. Rev.* **D42** (1990) 3660

[11] S. Coleman, R. Jackiw and H.D. Politzer, *Phys. Rev.* **D10** (1974) 2491
S. Coleman, *Aspects of Symmetry, Cambridge University Press*, (1985)

[12] R. Casalbuoni, D. Dominici and R. Gatto, *Phys. Lett.* **B147** (1984) 419
M.B. Einhorn, *Nucl. Phys.* **B246** (1984) 75

[13] M. S. Chanowitz, M. Golden and H. Georgi, *Phys. Rev.* **D36** (1987) 1490

[14] M.J. Dugan and M. Golden, *Phys. Rev.* **D48** (1993) 4375

[15] Y.P.Yao and C.P. Yuan, *Phys. Rev.* **D38** (1988) 2237

[16] G.P. Lepage, *J. Comput. Phys.* **27** (1978) 192

[17] S. Dawson, *Nucl. Phys.* **B249** (1985) 42

[18] C.Weizsaker and E.J.Williams, *Z. Phys.* **88** (1934) 612

[19] A.D. Martin, R.G Roberts and W.J. Stirling, *Phys. Lett.* **B306** (1993) 145 and *Phys. Lett.* **B309** (1993) 492

[20] E.W.N.Glover and J.J.Van deer Bij, *Nucl. Phys.* **B321** (1989) 561